Atomic Layer Deposition of Al_2O_3 Thin Films from a 1-Methoxy-2-methyl-2-propoxide Complex of Aluminum and Water

Yo-Sep Min,*[,†,‡] Young Jin Cho,[†] and Cheol Seong Hwang[‡]

Nano-Fabrication Center, Samsung Advanced Institute of Technology, Yong-In, Kyeongki-Do 449-712, and School of Materials Science and Engineering, Seoul National University, Seoul 151-742, Korea

Received August 14, 2004. Revised Manuscript Received November 1, 2004

Al_2O_3 thin films were grown by atomic layer deposition (ALD) using the novel volatile complex $Al(mmp)_3$ (mmp = 1-methoxy-2-methyl-2-propoxide, $OCMe_2CH_2OMe$) and water vapor in the temperature range of 200−450 °C on p-type Si or $Ru/SiO_2/Si$ substrates. Al_2O_3 films were formed at 250 °C through the typical self-limiting mechanism of ALD, wherein the saturated growth rate was about 0.6 Å/cycle. The resultant films were amorphous, and the refractive index of the films varied between 1.53 and 1.62, which was dependent on the growth temperature and water pulse length. The aluminum-to-oxygen ratio of the Al_2O_3 film grown at 250 °C was 2:3.1, and the carbon content was 2.4%. With capacitance−voltage measurements of $Al/Al_2O_3/SiO_2/Si$ structures, the dielectric constant of Al_2O_3 grown at 250 °C is evaluated to be 7.7, and the flat band voltage appears at 1.05 V, which corresponds to a negative fixed charge on the order of $10^{11}/cm^2$. The leakage current density of the Al_2O_3 films is on the order of 10^{-7} A/cm^2 at 1 MV/cm, and the dielectric breakdown voltage is about 6.5 MV/cm.

1. Introduction

Al_2O_3 films have attracted great interest as an alternative high-*k* dielectric material in ultra-large-scale integrated devices because of their excellent characteristics such as chemical and thermal stability, high dielectric constant (∼9), large band gap (8.7 eV), and high field strength (6−8 MV/cm).[1] In recent years, Al_2O_3 thin films as an alternative high-*k* dielectric for microelectronic devices have increasingly been deposited by atomic layer deposition (ALD), due to the ultrathin thickness of the insulating layer being thinner than 10 nm. Since Suntola, the pioneer of ALD, deposited Al_2O_3 by ALD,[2] Al_2O_3 thin films have been studied extensively with various precursors over the past several decades. For example, $AlCl_3$, aluminum ethoxide, aluminum *n*-propoxide, and trimethylaluminum (TMA) as an Al source, and oxygen, water, hydrogen peroxide, and ozone as an oxidant have all been studied.[2−6] Recent studies on ALD of Al_2O_3 films have been concentrated on the precursor system of TMA and water or ozone because reactions of TMA with water vapor or ozone are highly exothermic and occur readily with a low activation barrier.[7−12]

Among ligands for metal alkoxide precursors, a bifunctional 1-methoxy-2-methyl-2-propoxide ($OCMe_2CH_2OMe$, mmp) ligand has been applied to various metals such as Bi, Ti, Zr, Hf, La, and Pr.[13−20] The mmp ligands form relatively stable and highly volatile complexes especially with low charge-to-radius ratio metals due to O-donor functionalization.[21] These precursors are useful for the deposition of multicomponent oxides including low charge-to-radius ratio metals, since the liquid injection method, which is increasingly being used for low-volatility precursors, often uses a solution of each metal precursor for multicomponent films

* To whom correspondence should be addressed. E-mail: ysmin@sait.samsung.co.kr.
† Samsung Advanced Institute of Technology.
‡ Seoul National University.

(1) Lee, J. Y.; Lai, B. C. In *Handbook of Thin Film Materials*; Nalwa, H. S., Ed.; Academic Press: San Diego, 2002; Vol. 3, Chapter 1.
(2) Suntola, T.; Antson, J.; Pakkala, A.; Lindfors, S. *SID 80 Dig.* **1980**, *11*, 108.
(3) Ritala, M.; Leskela, M. In *Handbook of Thin Film Materials*; Nalwa, H. S., Ed.; Academic Press: San Diego 2002, Vol. 1, Chapter 2.
(4) Hiltunen, L.; Kattelus, H.; Leskela, M.; Makela, M.; Niinisto, L.; Nykanen, E.; Soininen, P.; Tiitta, M. *Mater. Chem. Phys.* **1991**, *28*, 379.
(5) Higashi, G. S.; Fleming, C. G. *Appl. Phys. Lett.* **1989**, *55*, 1963.
(6) Fan, J. F.; Sugioka, K.; Toyoda, K. *Jpn. J. Appl. Phys.* **1991**, *30*, L1139.
(7) Ott, A. W.; Klaus, J. W.; Johnson, J. M.; George, S. M. *Thin Solid Flims* **1997**, *292*, 135.
(8) Juppo, M.; Rahtu, A.; Ritala, M.; Leskela, M. *Langmuir* **2000**, *16*, 4034.
(9) Kim, J. B.; Kwon, D. R.; Chakrabarti, K.; Lee, C.; Oh, K. Y.; Lee, J. H. *J. Appl. Phys.* **2002**, *92*, 6739.
(10) Kim, J.; Chakrabarti, K.; Lee, J.; Oh, K. J.; Lee, C. *Mater. Chem. Phys.* **2003**, *78*, 733.
(11) Yang, W. S.; Kim, Y. K.; Yang, S. Y.; Choi, J. H.; Park, H. S.; Lee, S. I.; Yoo, J. B. *Surf. Coat. Technol.* **2000**, *131*, 79.
(12) Kim, S. K.; Hwang, C. S. *J. Appl. Phys.* **2004**, *96*, 2323.
(13) Min, Y. S.; Cho, J. Y.; Hwang, C. S. *Electrochem. Solid-State Lett.* **2004**, *7* (12), F85.
(14) Min, Y. S.; Cho, Y. J.; Asanov, I. P.; Han. J. H.; Kim, W. D.; Hwang, C. S. *Chem. Vap. Deposition* **2005**, *11*, in press.
(15) Kukli, K.; Ritala, M.; Leskela, M.; Sajavaara, T.; Keinonen, J.; Jones, A. C.; Roberts, J. L. *Chem. Mater.* **2003**, *15*, 1722.
(16) Williams, P. A.; Jones, A. C.; Crosbie, M. J.; Wright, P. J.; Bickely, J. F.; Steiner, A.; Davies, H. O.; Leedham, T. J.; Critchlow, G. W. *Chem. Vap. Deposition* **2001**, *7*, 205.
(17) Williams, P. A.; Jones, A. C.; Crosbie, M. J.; Wright, P. J.; Bickley, J. F.; Steiner, A.; Davies, H. O.; Leedham, T. J.; Critchlow, G. W. *Chem. Vap. Deposition* **2001**, *7*, 205.
(18) Wiliams, P. A.; Roberts, J. L.; Jones, A. C.; Chalker, P. R.; Tobin, N. L.; Bickley, J. F.; Davies, H. O.; Smith, L. M.; Leedham, T. J. *Chem. Vap. Deposition* **2002**, *8*, 163.
(19) Aspinall, H. C.; Gaskell, J.; Williams, P. A.; Jones, A. C.; Chalker, P. R.; Marshall, P. A.; Smith, L. M.; Critchlow, G. W. *Chem. Vap. Deposition* **2004**, *10*, 13.
(20) Aspinall, H. C.; Gaskell, J.; Williams, P. A.; Jones, A. C.; Chalker, P. R.; Marshall, P. A.; Smith, L. M.; Critchlow, G. W. *Chem. Vap. Deposition* **2004**, *10*, 83.
(21) Herrmann, W. A.; Huber, N. W.; Runte, O. *Angew. Chem., Int. Ed. Engl.* **1995**, *34*, 2187.

10.1021/cm048649g CCC: $30.25
Published on Web 01/07/2005

to precisely control the relative amount of them. Therefore, good precursor compatibility is especially important for ALD of multicomponent films.[22]

Recently, we reported a new class of amorphous high-*k* dielectric, $Bi_{1-x-y}Ti_xSi_yO_z$ (BTSO) thin films grown by ALD from $Bi(mmp)_3$, $Ti(mmp)_4$, and silicon tetraethoxysilane.[13,14] Silicon was added to make the BTSO amorphous and to obtain a low leakage current. However, since the dielectric constant of SiO_2 is only 3.9, the dielectric constant of BTSO is lowered with the addition of silicon. Aluminum oxide has a band gap (8.7 eV) comparable to that of SiO_2 (9.0 eV), but has a higher dielectric constant (9) than SiO_2.[1] To our knowledge, $Al(mmp)_3$ has not been studied yet as an ALD precursor. Although the TMA ALD process is well-established, $Al(mmp)_3$ is more proper in liquid injection ALD due to its better stability. In this study, Al_2O_3 thin films were grown from aluminum tris(1-methoxy-2-methyl-2-propoxide), $Al(mmp)_3$, and H_2O to investigate the ALD behavior of this new precursor combination as well as the dielectric properties of the resulting films.

2. Experimental Section

$Al(mmp)_3$ was dissolved in ethylcyclohexane (ECH) to obtain a 0.1 M precursor solution. Distilled water vapor was generated from an external reservoir at room temperature and led into the reaction chamber through solenoid valves without any carrier gas. Al_2O_3 thin films were grown on 8 in. diameter bare Si wafers or Ru (500 Å)/SiO_2 (1000 Å)/Si substrates. The native oxide of the bare wafers was not removed before the deposition.

ALD was carried out in a laminar flow type reactor (FELFRA 7201, Moohan Co., Ltd.), which minimizes the ALD reaction volume. The deposition system can process four 8 in. wafers at the same time on a rotating substrate holder (five rotations per minute) heated with halogen lamps.

The liquid delivery technique via a commercial automobile fuel injector was adopted in this study for the stable and precise supply of $Al(mmp)_3$/ECH solution. The precursor solution was contained in a canister that was pressurized with Ar gas to deliver the precursor solution into a liquid injector. The liquid injector was connected to a vaporizer, which was attached to a reactor. The vaporizer temperature was kept at 200 °C. When the injector was turned on, about 0.014 mL (1.4×10^{-6} mol/injection) of the precursor solution was injected and carried by an Ar gas (1000 sccm) to the reactor. The feeding amount of the metal precursor was controlled by the number of injections for 1 s, which was varied between one and seven. The water pulse length was normally 2.0 s with a dose of 1.1×10^{-4} mol/s except for the experiments in which the growth rate was obtained as a function of water pulse length in the range of 0.2−3.0 s. A constant Ar gas (1600 sccm) purge of 5 s was used after each precursor pulse to remove volatile byproducts and any excess reactants in the reactor. The working pressure was about 1.8−2.5 Torr in the source injection step and about 0.7−0.8 Torr in all of the other steps.

The film thickness was determined by a spectroscopic ellipsometer (J. A. Woollam Co., Inc.) with a Cauchy dispersion model. X-ray diffraction (XRD) measurements were carried out in $\theta/2\theta$ scan mode using a Philips X'pert Pro MRD X-ray diffractometer with Cu Kα radiation. Low-angle X-ray reflectivity (XRR) data were collected in 0.005° increments and 2 s count times. XRR data were analyzed with the WinGixa program, provided by Philips. X-ray photoelectron spectroscopy (XPS) spectra were measured on a Quantum 200 scanning microprobe spectrometer using monochromatic Al Kα emission. Binding energies were measured using the C 1s peak (284.8 eV) of the adventitious carbon as an internal standard. Sputtering during XPS was performed with 0.5 keV Ar^+ ions.

A 200 nm thick Al top electrode was deposited onto the Al_2O_3/SiO_2/p-Si structure with a shadow mask (hole diameter 300 μm) by e-beam evaporation. The thickness of the Al_2O_3 film was 320 Å. Silver paste was applied between the backside of the sample and another Si wafer to obtain ohmic contact. The sample was finally annealed at 400 °C in a N_2 atmosphere for 20 min. Current−voltage ($I-V$) and capacitance−voltage ($C-V$) characteristics were measured by a Keithley 236 source measurement unit and a Precision LCR meter (HP 4284A) at 10 kHz, respectively.

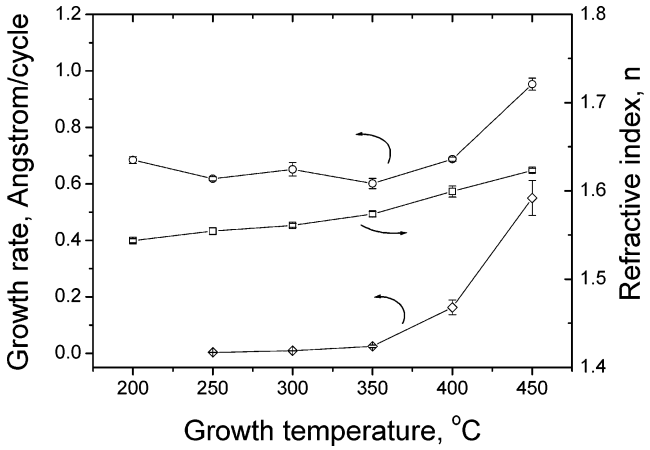

Figure 1. Growth rate (circles) and refractive index (squares) of Al_2O_3 films grown on Si(100) as a function of growth temperature. The precursor solution was injected five times for 1 s, and the H_2O pulse length was 2 s. The purge time after the precursor or water pulse was 5 s. The error bars express the variation of the growth rate and refractive index in each sample over an 8 in. substrate. The tilted square symbols indicate the growth rate in the absence of water pulse steps.

3. Results and Discussion

3.1. Film Growth and Characterization. The variation in growth rate of Al_2O_3 films grown on Si(100) wafers from $Al(mmp)_3$ and H_2O was plotted as a function of the growth temperature in Figure 1 (circles). It can be seen that the growth rate is kept nearly constant in a range of 0.6−0.7 Å/cycle from 200 to 350 °C, and then increases above 350 °C. To identify the growth temperature window for ALD, Al_2O_3 growths were also performed without water vapor in the temperature range of 250−450 °C, and the growth rates are plotted in Figure 1 as tilted squares. Al_2O_3 films were not actually grown below 350 °C but grown above 350 °C without the water pulse step owing to the self-decomposition of the Al precursors. The ALD window is at a temperature range of 250−350 °C, wherein the growth rate is nearly constant regardless of the growth temperature and there is no thermal decomposition. Above 350 °C, the self-decomposition of the $Al(mmp)_3$ complex coincides with a report on bismuth oxide growth from $Bi(mmp)_3$ at 350 °C without any additional oxidants due to the provision of excess oxygen by the bifunctional mmp ligand.[16] In comparison with the growth rate (0.8−1.1 Å/cycle) of Al_2O_3 from TMA and

(22) Jones, A. C.; Williams, P. A.; Tobin, N. L.; Chalker, P. R.; Marshall, P.; Wright, P. J.; Lane, P. A.; Donohue, P.; Smith, L. M.; Davies, H. O. *Electrochem. Soc. Proc.* **2003**, *2003−08*, 871.

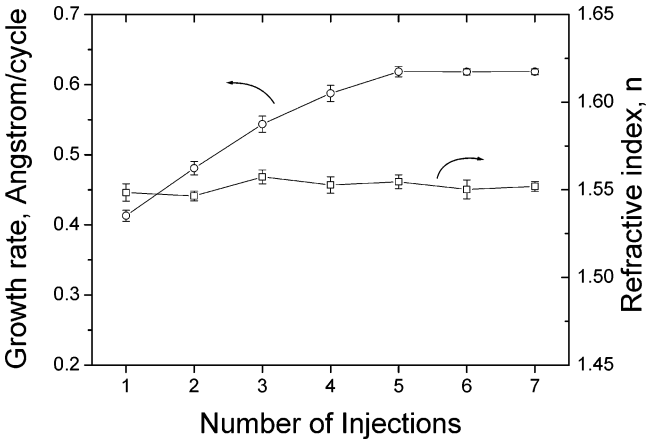

Figure 2. Growth rate (circles) and refractive index (squares) of Al_2O_3 films grown on Si(100) at 250 °C as a function of the number of precursor injections. The precursor injection was performed in 1 s, and the H_2O pulse length was 2 s. The purge time after the precursor or water pulse was 5 s. The error bars express the variation of the growth rate and refractive index in each sample over an 8 in. substrate.

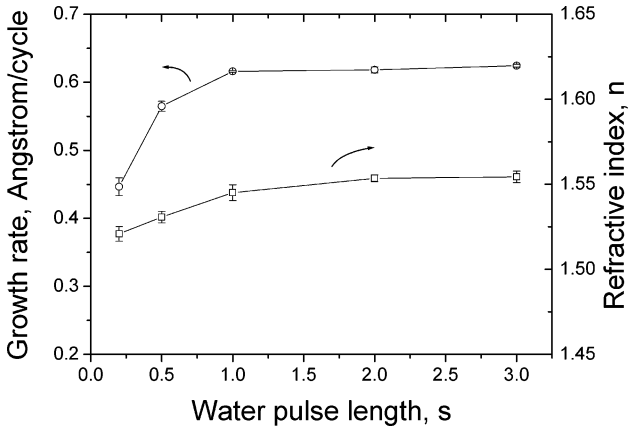

Figure 3. Growth rate (circles) and refractive index (squares) of Al_2O_3 films grown on Si(100) at 250 °C as a function of water pulse length. The precursor injection rate was six injections per second. The purge time after the precursor or water pulse was 5 s. The error bars express the variation of the growth rate and refractive index in each sample over an 8 in. substrate.

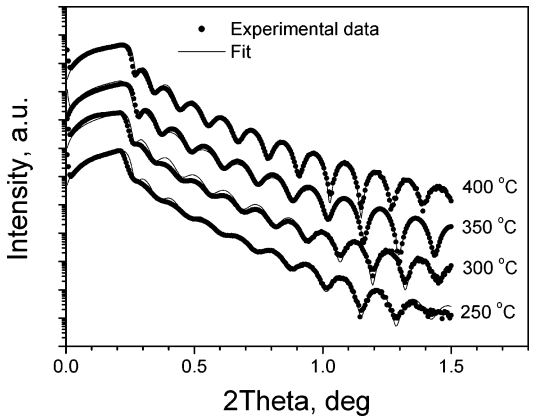

Figure 4. XRR scans for Al_2O_3 films on Si(100) at a growth temperature from 250 to 400 °C.

water,[7] the lower growth rate from $Al(mmp)_3$ is probably due to the bulky structure of $Al(mmp)_3$, since bulkier ligands of the chemisorbed $Al(mmp)_3$ shield a greater part of the growing surface from the other $Al(mmp)_3$ molecules.[23] The molecular weight of $Al(mmp)_3$ is 4.7 times larger than that of TMA.

The refractive index of the films monotonically increases from 1.55 to 1.62 with the growth temperature as shown in Figure 1 (squares). However, even at the highest growth temperature studied, the refractive index is lower than that of bulk α-Al_2O_3 (corundum, 1.76−1.77), the density of which is 3.97 g/cm^3.[24] The lower refractive index may be due to some impurities and the amorphous structure of the films. It is noted that the films can contain hydrogen, excess oxygen, and carbon, which may arise from the hydroxyl groups, the excess water, or the unreacted ligands in the films. For example, aluminum oxyhydroxide (AlO(OH), boehmite) has a lower refractive index (1.64−1.66) and lower density (3.44 g/cm^3) than α-Al_2O_3.[24] It is also reported that the amorphous Al_2O_3 films grown from TMA and water also show a monotonically increasing refractive index of 1.51−1.60 in a growth temperature range of 33−177 °C.[25]

Figures 2 and 3 (circles) show the growth of Al_2O_3 films is self-limiting as the supplied amount of Al precursor or water vapor increases. At over five injections of Al precursor (7.0×10^{-6} mol) and a 1 s water pulse length (1.1×10^{-4} mol), the growth rate saturates at 0.62 Å/cycle. Recently, it was reported that adsorption of $Hf(mmp)_4$ was not entirely self-limiting at 360 °C in ALD of HfO_2 films from $Hf(mmp)_4$ and water, probably because of the thermal decomposition of the precursors.[15] HfO_2 films show a strong dependence of growth rate on the growth temperature above 350 °C, but a weak dependence with a growth rate of 0.3 Å/cycle in a growth temperature range of 300−325 °C. Such a non-self-limiting growth behavior of $Hf(mmp)_4$ is attributed to the high growth temperature (360 °C) at which thermal decomposition contributes to the film growth.

The effect of the number of $Al(mmp)_3$ injections and water pulse length on the refractive index of Al_2O_3 was also examined at 250 °C as shown in Figures 2 and 3 (squares). The refractive index is not dependent on the number of precursor injections but is weakly dependent on the water pulse length. As the water pulse length increases, the refractive index also increases and then saturates above 1 s, showing a shape similar to that of the curve of growth rate versus water pulse time. However, the amount of the supplied $Al(mmp)_3$ does not influence the refractive index.

Figure 4 shows XRR scans for Al_2O_3 films grown on Si(100) at growth temperatures from 250 to 400 °C with fitted data to determine the densities of the films. The density of Al_2O_3 increased from 2.83 g/cm^3 at 250 °C to 3.08 g/cm^3 at 400 °C. Even considering that the grown films are amorphous (data not shown), the densities are too low in comparison with the bulk value (3.97 g/cm^3). These low densities are probably due to carbon and hydrogen contaminants or excess oxygen in the films. The contaminants and excess oxygen may be incorporated into Al_2O_3 films by incomplete oxidation and local formation of aluminum hydroxide ($Al(OH)_3$) and aluminum oxyhydroxide, the densities of which are 2.42 and 3.44 g/cm^3, respectively. Recently, George et al. reported low densities (2.5−3.0

(23) Puurunen, R. L. *Chem. Vap. Deposition* **2003**, *9*, 249.
(24) *CRC Handbook of Chemistry and Physics*; CRC Press: Boca Raton, FL, 2000; pp 4−141.
(25) Groner, M. D.; Fabreguette, F. H.; Elam, J. W. George, S. M. *Chem. Mater.* **2004**, *16*, 639.

g/cm^3) for an amorphous Al_2O_3 film grown at low temperatures from 33 to 177 °C.[25] It was also reported that amorphous Al_2O_3 films deposited by dc magnetron sputtering have a density of 2.7 g/cm^3 due to the porous microstructure.[26]

The relationship between density and refractive index can be formulated with the Gladstone−Dale equation,[27] $\rho = K_1(n - 1)$, or the Lorentz−Lorenz formula,[28] $\rho = K_2(n^2 - 1)/(n^2 + 2)$, where ρ is the density, n is the refractive index, and K_1 and K_2 are constants. This means the refractive index is linearly related to the film density.[29,30] The refractive index correlation with the amounts of Al precursor and water shown in Figures 2 and 3, respectively, can be explained with density variation of the grown films. A sufficient supply of water may be more important to obtain a dense film than that of Al(mmp)$_3$. The insufficient supply of oxidant gas may cause severe carbon contaminants in films, but that of Al precursor only lowers the growth rate.

The film density can be used to estimate the thickness of one Al_2O_3 layer.[7] The density (2.83 g/cm^3) at 250 °C corresponds to a number density of $n = 1.67 \times 10^{22}$ Al_2O_3 units/cm^3. The thickness (d) of one monolayer can be estimated using $d \approx n^{-1/3} = 3.91$ Å. This approximation is reasonable because the films are amorphous. Considering the growth rate (0.62 Å/cycle) at 250 °C, six or seven reaction cycles are necessary to grow one monolayer of Al_2O_3 unit.

On the mechanism of incorporation and desorption of Hf(mmp)$_4$ during metal−organic chemical vapor deposition (MOCVD) of HfO_2 films, it was reported that 1-methoxy-2-methyl-1-propene [Me$_2$C═CHOCMe] was generated through the breaking of the HfO−C bond and the elimination of β-hydrogen in the mmp ligand during gas chromatography−mass spectrometry (GC−MS) of Hf(mmp)$_4$.[31] Since the central Al^{3+} ion of Al(mmp)$_3$ is sterically hindered from the direct attack of the surface hydroxyl groups by the bulky mmp ligands, it is expected that the proposed reaction generating 1-methoxy-2-methyl-1-propene may take part in the adsorption reaction of Al(mmp)$_3$ on the hydroxyl surface. However, for a more detailed mechanism, a further study should be performed.

Figure 5 shows the XPS of Al 2p (top) and O 1s (bottom) core levels obtained from the depth profile of the Al_2O_3 film grown at 250 °C. Before the removal of adventitious carbons from the surface, the Al 2p and O 1s peaks were located at 74.8 and 531.6 eV, respectively. After sputtering with Ar^+ of 0.5 keV for 1 min, the aforementioned peaks were shifted to 75.5 and 532.4 eV, respectively, and there was no significant shifting during depth profiling. According to some recent reports,[9−11] Al_2O_3 films from TMA and water show

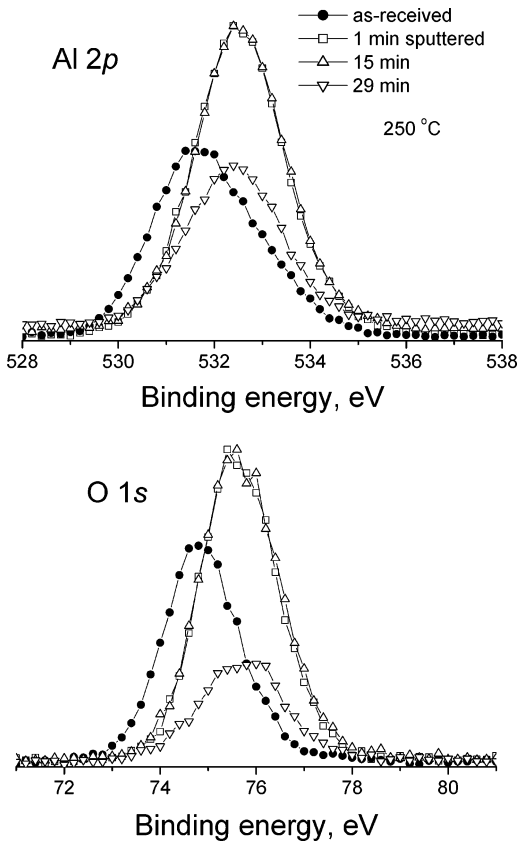

Figure 5. Al 2p (top) and O 1s (bottom) core level photoemission spectra of Al_2O_3 films grown on Si(100) at 250 °C.

Table 1. Binding Energies (eV)[a,b] of 1 min Sputtered and As-Received Al_2O_3 Films and a Single Crystal of α-Al_2O_3 (Sapphire)

T_{growth} (°C)	Al 2p	O 1s	O 1s−Al 2p
250	75.5 (74.8)[c]	532.4 (531.6)	456.9 (456.8)
300	74.8 (74.4)	531.6 (531.4)	456.8 (457.0)
350	75.3 (74.7)	532.2 (531.5)	456.9 (456.8)
400	75.5 (74.5)	532.3 (531.3)	456.8 (456.8)
sapphire	74.3 (74.3)	531.0 (531.1)	456.7 (456.8)

[a] The binding energies were referenced to C 1s at 284.8 eV. [b] The spectra were obtained with 0.2 eV steps. [c] All of the values in parentheses were obtained from as-received samples.

the low binding energy peak (72.8 eV) near the interface region, corresponding to Al−Al bonds. That peak is reduced or disappears in Al_2O_3 films grown from TMA and ozone. However, the Al−Al peak does not appear in the Al_2O_3 film from Al(mmp)$_3$, even with the water process.

Table 1 summarizes the binding energies of Al_2O_3 films grown in the temperature range of 250−400 °C in comparison with those of sapphire (α-Al_2O_3). The Al 2p and O 1s core level photoemissions of sapphire are located at 74.3 and 531.0 eV, respectively. These binding energies are in good agreement with some published data for α-Al_2O_3.[32−34] However, the binding energies of Al 2p and O 1s in the Al_2O_3 films studied appear at higher binding energy positions, regardless of the growth temperature. In recent reports, there have been mutually contradictory assignments of the Al 2p

(26) Drusedau, T. P.; Neubert, T.; Panckow, A. N. *Surf. Coat. Technol.* **2003**, *163−164*, 164.
(27) Gladstone, J. H.; Dale, T. P. *Philos. Trans. R. Soc. London* **1863**, *153*, 317.
(28) Born, M.; Wolf, E. *Principles of Optics*, 7th ed.; Cambridge University Press: Cambridge, U.K., 1999; p 89.
(29) Pliskin, W. A. *J. Vac. Sci. Technol.* **1977**, *14*, 1064.
(30) Alonso, J. C.; Vazquez, R.; Ortiz, A.; Pankov, V.; Andrade, E. *J. Vac. Sci. Technol., A* **1998**, *16*, 3211.
(31) Horri, S.; Yamamoto, K.; Asai, M.; Miya, H. Niwa, M. *Jpn. J. Appl. Phys.* **2003**, *42*, 5176.
(32) Madey, T. E.; Wagner, C. D.; Joshi, A. *J. Electron Spectrosc. Relat. Phenom.* **1977**, *10*, 359.
(33) Paparazzo, E. *Appl. Surf. Sci.* **1986**, *25*, 1.
(34) Tayloer, J. A. *J. Vac. Sci. Technol.* **1982**, *20*, 751.

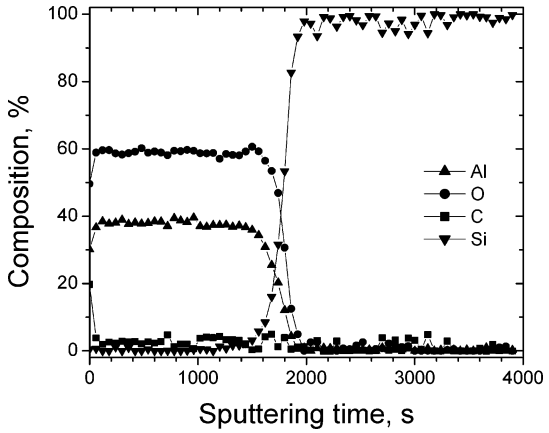

Figure 6. XPS depth profile of Al_2O_3 films grown on Si(100) at 250 °C.

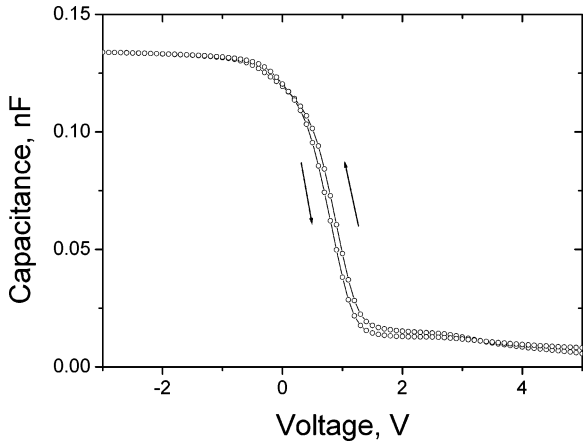

Figure 7. Capacitance−voltage curve measured from an Al/Al_2O_3/SiO_2/p-Si capacitor at an ac signal frequency of 1 MHz.

peaks for Al_2O_3 or suboxides. Some papers report the Al 2p peak shifts from high to low binding energy corresponding to a conversion from substoichiometric Al_2O_{3-x} to Al_2O_3,[34,35] though other studies assign a shift to higher binding energies for increasing O in Al_2O_{3-x}.[36] Since the surface Fermi level of Al_2O_3 can be altered by the overall film chemistry, including the presence of low-level impurities, it was recently proposed that the binding energy of photoelectrons from atoms with the same local chemical environment was altered by this effect.[37−39] Thus, positions for a given chemical environment may not be determined uniquely by charge correction using the C 1s peak; instead, the O 1s components must be defined relative to the Al 2p peak. Therefore, it should be noted that the energy spacing between the Al 2p and O 1s peaks is about 456.7−457.0 eV in all of the Al_2O_3 films and the sapphire wafer regardless of the removal of the adventitious carbon. This means that there is no significant difference between the Al oxidation state of Al_2O_3 grown from Al(mmp)$_3$ and that of sapphire.

Figure 6 shows an XPS depth profile of an Al_2O_3 film grown on Si at 250 °C. The composition of each element in Al_2O_3 films was calibrated with that of sapphire (O/Al = 1.5). After the removal of the adventitious carbon, the composition of each element was constant over the film depth. The aluminum-to-oxygen ratio of the Al_2O_3 film was 2:3.1, and the carbon content was 2.4%. The excess oxygen in the film is probably due to a small portion of AlO(OH) and/or alkoxy residues. The carbon residue decreases with increasing growth temperature, and the carbon content in Al_2O_3 grown at 400 °C is less than 0.5%.

3.2. Electrical Properties. Figure 7 shows a $C-V$ curve at 1 MHz for an Al/Al_2O_3/SiO_2/p-Si(100) metal−insulator−silicon (MIS) structure with the Al_2O_3 film (320 Å) grown at 250 °C. The capacitor area was 7.1×10^{-4} cm^2, defined by using a shadow mask during Al deposition. It shows the typical features of an n-type metal oxide semiconductor (n-MOS) capacitor with an accumulation region at negative biases and an inversion region at positive biases.[40−42] The variation of capacitance as the bias increases is caused by changes in the thickness of the carrier depletion region of the p-Si substrate. At large negative biases where the silicon surface is in accumulation, the measured capacitance is approximately equal to the serial capacitance of the grown Al_2O_3 and native SiO_2 layers. Considering a measured 20 Å thick native oxide, the dielectric constant of which is 3.9, the estimated dielectric constant of the Al_2O_3 films is 7.7 from the serial capacitance equation $1/C = 1/C_{SO} + 1/C_{AO}$, where C is the measured capacitance at the accumulation region (−3 V) and C_{SO} and C_{AO} are the capacitances from SiO_2 and Al_2O_3, respectively. This value is lower than ∼9 which is usually reported,[1] since the grown Al_2O_3 films contain impurities as mentioned above.

It should be noted on the $C-V$ curve that the depletion region appears at positive bias even though it is expected at negative bias.[5,43] Considering the resistivity (2−20 Ω cm) of p-Si used, the doping concentration of p-Si is $\sim 1 \times 10^{15}$/cm^3.[40] The work function difference (ϕ_{MS}) of Al and p-Si is evaluated to be around −0.9 to −1.1 eV.[44] If there is no oxide charge in this capacitor, the flat band voltage (V_{FB}) is equal to ϕ_{MS} for the aluminum and silicon substrate. However, as shown in Figure 7, V_{FB} was determined to be 1.05 eV from the flat band capacitance (C_{FB}) of 0.04 nF, which was calculated from the equation $C_{FB} = 1/(1/C + L_D/A\epsilon_s)$, where A is the area of the capacitor (7.1×10^{-4} cm^2), L_D is the Debye length (0.13 μm at a doping concentration of 1×10^{15} cm^{-3}), and ϵ_s is the permittivity ($11.9 \times 8.854 \times 10^{-14}$ F/cm) of silicon.[42] Since the parallel shift of the $C-V$ curve is attributed to fixed charges (Q_f), which are located at or very near the interface of the dielectric and silicon, the positive flat band voltage shift ($\Delta V_{FB} = 1.95-2.15$ V) corresponds to a negative fixed charge density

(35) Kottler, V.; Gillies, M. F.; Kuiper, A. E. T. *J. Appl. Phys.* **2001**, *89*, 3301.
(36) Faraci, G.; La Rosa, S.; Pennisi, A. R.; Hwu, Y.; Margaritondo, G. *J. Appl. Phys.* **1995**. *78*, 4091.
(37) Mullins, W. M.; Averbach, B. L. *Surf. Sci.* **1988**, *206*, 41.
(38) Mullins, W. M.; Averbach, B. L. *Surf. Sci.* **1988**, *206*, 52.
(39) Alexsander, M. R.; Thompson, G. E.; Beamson, G. *Surf. Interface Anal.* **2000**, *29*, 468.
(40) Sze, S. M. *Physics of Semiconductor Devices*, 2nd ed.; Wiley and Sons: New York, 1981; p 32.
(41) Schroder, D. K. *Semiconductor Material and Device Characterization*, 2nd ed.; Wiley and Sons: New York, 1998; p 360.
(42) Hori, T. *Gate Dielectrics and MOS ULSIs*; Springer: Berlin, 1997; p 23.
(43) Ishida, M.; Katakabe, I.; Nakamura, T. *Appl. Phys. Lett.* **1988**, *52*, 1326.
(44) Johnson, R. S.; Lucovsky, G.; Baumvol, I. *J. Vac. Sci. Technol., A* **2001**, *19*, 1353.

($N_f = Q_f/q$) of $6.9 \times 10^{11}/cm^2$ to $7.6 \times 10^{11}/cm^2$, which can be calculated by multiplying $\Delta V_{FB}/q$ by the flat band capacitance density (C_{FB}/A), where q is the elementary charge.[42] Since the N_f of the SiO_2/Si interface is usually low (a few $10^{10}/cm^2$) enough to be negligible compared to the measured value, it is believed that the negative fixed charges are mainly located at the Al_2O_3/SiO_2 interface. Recently, Johnson et al. also reported a negative fixed charge ($7.0 \times 10^{12}/cm^2$) for $Al/Al_2O_3/SiO_2$/Si capacitors by a plot of V_{FB} and equivalent oxide thickness.[44] They explained tetrahedrally coordinated Al sites having a net negative charge among the local atomic bonding of noncrystalline Al_2O_3 are responsible for the negative fixed charge.

One more concern of the $C-V$ curve is the anticlockwise hysteresis with a hysteresis voltage (V_{hy}) of 0.1 V as shown in Figure 7, which is generally attributed to trapped charges in the bulk of the oxide.[41] The hysteresis appears in an anticlockwise manner regardless of the sweep directions. Therefore, the hysteresis is mainly due to the electrons trapped in the bulk of the oxide.

Figure 8 shows the current density−electric field ($J-E$) curve of the Al_2O_3 film grown on p-Si at 250 °C. Here, the electric field was calculated by simply dividing the applied voltage by the total oxide thickness of Al_2O_3 (320 Å) and native SiO_2 (20 Å) measured by a spectroscopic ellipsometer. The leakage current density is about 1×10^{-7} A/cm^2 at 1 MV, which is higher than $10^{-8}-10^{-9}$ A/cm^2 of the Al_2O_3 films grown from TMA and water.[9,45] This may be due to the remaining impurities in the film, such as carbon as mentioned above. The dielectric breakdown appeared at ~6.5 MV/cm, which is well consistent with reported values (6−8 MV/cm).[1,45]

(45) Groner, M. D.; Elam, J. W. Fabreguette, F. H. George, S. M. *Thin Solid Films* **2002**, *413*, 186.

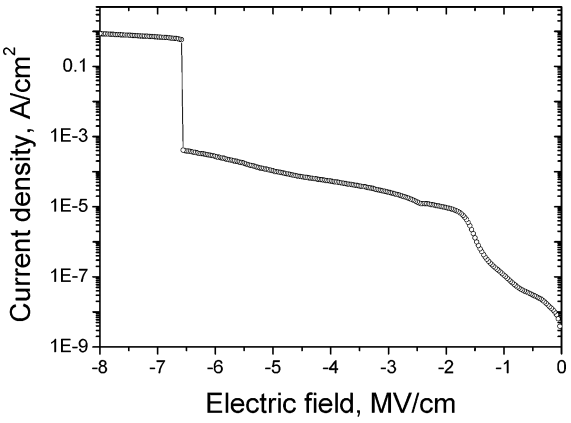

Figure 8. Current density−electric field curve measured from an $Al/Al_2O_3/SiO_2$/p-Si capacitor.

4. Conclusion

Al_2O_3 thin films were successfully grown from $Al(mmp)_3$ and water at 250 °C through the typical self-limiting mechanism of ALD, wherein the saturated growth rate was about 0.6 Å/cycle, although the films from $Al(mmp)_3$ are inferior to those from TMA. The refractive index of the resultant amorphous films varies between 1.53 and 1.62 depending on the growth temperature and water pulse length. The aluminum-to-oxygen ratio of Al_2O_3 films grown at 250 °C is 2:3.1, and the carbon content is 2.4%. By $C-V$ measurements from an $Al/Al_2O_3/SiO_2$/Si capacitor, the dielectric constant of Al_2O_3 grown at 250 °C is evaluated to be 7.7, and the fixed charge density is on the order of $10^{12}/cm^2$. The leakage current density of Al_2O_3 films is 1×10^{-7} A/cm^2 at 1 MV/cm, and the dielectric breakdown field is ~6.5 MV/cm.

Acknowledgment. This work was partially supported by the System IC 2010 project of the Korean government.

CM048649G